Longitudinal and Transverse Interactions between Stacked Parallel Tunnels Constructed using Shield Tunnelling in Residual Soil

C.W. Boon[1] and L.H. Ooi[1]
[1]*MMC-Gamuda KVMRT(T) Sdn Bhd, Kuala Lumpur, Malaysia*
E-mail: cwboon@kvmrt-ug.com.my

ABSTRACT: In the construction of stacked parallel twin tunnels, the lower tunnel is normally constructed first before the upper tunnel to minimise the impact to the first tunnel due to the construction of the second tunnel. This paper examines the special case in which the upper tunnel was constructed first and undermined subsequently in a parallel configuration during the construction of the lower tunnel using shield tunnelling in residual soil. The longitudinal settlement profile of the upper tunnel due to the undermining by the lower tunnel was studied analytically using Winkler beam solutions, and the results were compared with field measurements through a case history. As the twin tunnels transitioned from a stacked configuration into a skewed configuration, the settlement of the upper tunnel was studied using several common solutions in engineering practice, such as cavity expansion, Gaussian settlement solutions and finite element analyses. The discrepancies between the closed-form solutions and field measurements were found to be largely due to the influence of the lateral earth pressure coefficient, K_0<1. According to the finite element analyses, the in-situ stresses with K_0<1 had a competing deformation mechanism with the settlements induced by tunnelling volume losses. Comparison was carried out against the conventional tunnelling sequence in which the lower tunnel was constructed first, the results of which revealed deformation magnitudes more than five times smaller, underscoring the need for detailed analyses for tunnelling sequences in which an existing tunnel is undermined. Equations to estimate the subsurface Gaussian trough width parameter from a pair of extensometer readings were derived and presented in the Appendix. Nonetheless, the extensometer measurements were localised and may not be representative of the entire geological formation.

KEYWORDS: Tunnel interaction, Stress ratio, Winkler beam, Undermining, Settlement

1. INTRODUCTION

The construction of stacked twin tunnels is common due to the tight corridors which are free-of-obstruction and available for tunnelling in a built-up urban environment. To minimise the risks related to tunnel interactions between a pair of stacked twin tunnels during construction, the lower tunnel is normally constructed first before the upper tunnel. This paper presents a study on the special case, in which the upper tunnel is constructed first before the lower tunnel. As the underground section of a mass rapid transit (MRT) line typically consists of several launching, retrieval, pull-through, bore-through stations or shafts, the impact of the adopted excavation and tunnelling sequence interfacing with each other is non-trivial, and it is in the interest of the design and build contractor to be able to evaluate and mitigate the risks involved (Boon et al., 2016). The construction of the upper tunnel before the lower tunnel may arise due to the interfacing of tunnel construction with the excavations of launching shafts. The undermining of an existing tunnel may also occur when a new MRT tunnel needs to go underneath an existing tunnel in a parallel configuration.

Numerous studies are available in the literature concerning the interactions between twin tunnels (Liu et al., 2008; Hage Chehade & Shahrour, 2008; Chen et al., 2011; Do et al., 2014; Yamaguchi et al., 1998; Chu et al., 2007). There are also studies of twin tunnels undermining an existing structure (Afifipour et al., 2011; Mirhabibi & Soroush, 2012; Burd et al., 2000). Centrifuge studies have also been carried out by some investigators (Ng et al., 2013; Boonyarak et al., 2015; Ng et al., 2017). On the study of tunnelling impact to pre-existing tunnels, most studies are limited to local existing stretches of tunnels being subjected to undermining (Fang et al., 2015; Li & Yuan, 2012; Liu et al., 2011; Liu et al., 2009; Chakeri et al., 2011; Mohamad, 2010). It is difficult to draw general conclusions as regards the implications of constructing a pair of stacked twin tunnels with the construction sequence that the upper tunnel is constructed first, and undermined subsequently in a parallel manner by the lower tunnel. Some studies have been carried out with this construction sequence. A case history in Tokyo is reported in Taniguchi (2010) with brief discussions. The findings of Fang et al. (2016) focussed primarily on the ground surface settlements, whereas the results of Addenbrooke & Potts (2001) covered spatial configurations comprising purely stacked or purely side-by-side under plane strain conditions.

It is shown in this paper that the longitudinal settlement profile of the upper tunnel induced by the construction of the lower tunnel using shield tunnelling could be studied from a Winkler beam perspective. An attempt was made to compare the proposed solutions with field measurements with respect to the TBM face position. Further, to account for the influence of the launching shaft, the Winkler beam solution was adapted to include boundary conditions with fixity at one end, since the first ring is normally keyed into the retaining wall.

The field measurements as the twin tunnels departed from the purely stacked configuration, were compared with (i) cavity expansion solutions, (ii) volume loss methods to predict sub-surface Gaussian settlement profiles (Mair et al., 1993; Loganathan & Poulos, 1998) and (iii) finite element analyses. The influence of in-situ stresses was studied using finite element analyses and compared with closed-form solutions assuming isotropic stresses.

2. METHODOLOGY AND ANALYSES

The methods of analyses are explained in this Section, before discussing the case history in Section 3 and the results in Section 4.

2.1 Longitudinal Displacement Profile Using Winkler Beam Solution

Based on the assumption that the upper tunnel behaves like a beam and the soil as an elastic foundation, the deflection profile of the upper tunnel due to the undermining of the lower tunnel is tractable mathematically using the Winkler beam framework. It is noteworthy that the Winkler beam approach has been applied to study the response of pipelines, where tunnelling occurs underneath it and in a perpendicular direction to the axes of the pipelines (Klar et al., 2005; Marshall et al., 2010). The Winkler beam solution was also adopted to study the response of structures due to tunnelling (Franza et al., 2016). Unlike the aforementioned studies, the Winkler beam theory is applied in this paper to parallel tunnels which are stacked directly, one above the other. The solutions here provide the deflection profile normalised by the maximum settlement along the tunnel alignment. The subgrade stiffness and

the bending stiffness of the Winkler beam govern the shape of the longitudinal settlement profile, whereas the magnitudes of settlements can be obtained from other analytical methods, which are discussed later in Section 2.2. More rigorous analytical solutions based on the Winkler beam theory was presented by Kouretzis et al. (2015), which considered the influence of axial elongation and the resistance of the soil acting on the crown of pipelines due to heaving. These factors are assumed to be negligible in the analysis presented in this paper, since heaving is small by comparison to the magnitudes of settlement. The influence of elongation and shortening of the tunnel in the longitudinal direction were also assumed to be negligible since the magnitudes of soil movement are small by comparison to the diameter of the tunnel.

2.1.1 Boundary conditions of an infinite beam

The proposed Winkler beam solution assumes that there is loss of "support" behind the TBM shield, where there is normally a gap between the excavated opening and the lining which is grouted from the end of the TBM tailskin. Note that the loss of support considered here is analogous to the application of loads based on the conventional derivation of Winkler beam solutions (see Figure 1 (a)). For an infinite Winkler beam with (i) a constant load applied in the negative-x direction only, and with (ii) the boundary conditions of the displacements at the negative and positive far-ends being S_0 and nil respectively, the displacements along the beam can be expressed as (refer to Den Hartog (1952) on the Winkler beam theory):

$$S_{\text{back}} = S_0\left(1 - 0.5e^{-\beta x}\cos\beta x\right) \text{ for } S_0 \le 0 \quad (1)$$

$$S_{\text{front}} = S_0\left(0.5e^{-\beta x}\cos\beta x\right) \text{ for } S_0 \le 0 \quad (2)$$

where the origin of x is taken to be at the end of the TBM tailskin, S_0 is the maximum settlement along the longitudinal profile at negative far-end, and

$$\beta = \sqrt[4]{\frac{K_w}{4E_{\text{lining}}I_{\text{lining}}}} \quad (3)$$

$$k_w = \frac{0.65}{2a}\sqrt[12]{\frac{E_{\text{soil}}(2a)^4}{E_{\text{lining}}I_{\text{lining}}}\left(\frac{E_{\text{soil}}}{1-\nu^2}\right)} \quad (4)$$

where K_w=k_w(2a) is the subgrade stiffness taking into account the beam width for Winkler beam analysis, E_{lining} is the lining's Young's modulus, E_{soil} is the Young's modulus of the soil, ν is the Poisson's ratio, a is the radius of the tunnel. The subgrade stiffness, k_w, can be calculated using the solution in Vesic (1961) as a first approximation, and I_{lining} is the second moment of area of the cylinder (cross-section perpendicular to the tunnel axes). S_0 can be calculated either from an assumed volume loss induced by tunnelling (Peck, 1969), or as p/k_w where p is the loss in internal pressures due to tunnelling. The former approach is more straightforward.

The full derivation of Eq. (1) and (2) are available in Den Hartog (1952) and are not reproduced here. In Winkler beam theory, the two separate equations for the settlement profile in the positive and negative x-directions (S_{front} and S_{back}) result in S=0.5S_0 at x = 0. The choice of placing x = 0 at the TBM tailskin appears to be well suited to shield tunnelling, as the total magnitude of settlement at the end of TBM shield is approximately in the range of 50% of the total settlement (Thewes & Budach, 2009).

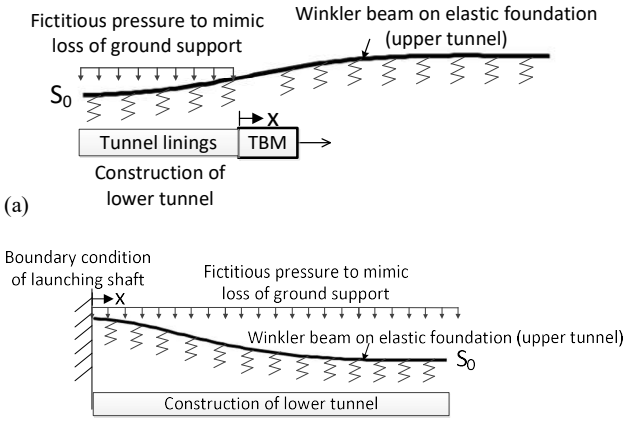

Figure 1 Winkler beam analogies for (a) longitudinal settlement profile, and (b) the influence of launching shaft

2.1.2 End boundary condition with influence of launching shaft

The influence of support afforded at the launching shaft to the longitudinal settlement profile of the tunnel may be significant as the first segment is typically keyed partially into the retaining wall of the launching shaft. This could be analysed from a Winkler beam perspective where fixity is introduced as a boundary condition at one end of the beam (see Figure 1 (b)). Two boundary conditions are explored, namely pinned-end and fixed-end respectively. The equations are as follows:

$$S_{\text{pinned}} = S_0\left(1 - e^{-\beta x}\cos\beta x\right) \text{ for } S_0 \le 0 \quad (5)$$

$$S_{\text{fixed}} = S_0\left(1 - e^{-\beta x}\left(\cos\beta x + \sin\beta x\right)\right) \text{ for } S_0 \le 0 \quad (6)$$

for pinned-end and fixed-end conditions respectively. The derivations of the equations are detailed in Appendix A.

2.2 Transition from stacked to side-by-side

Several well-known methods in the literature were adopted to predict the displacements induced by undermining, namely (i) cavity expansion solutions, (ii) sub-surface Gaussian settlement profile (Peck, 1969), and (iii) finite element analysis. The purpose of this comparison exercise, i.e. using different solutions (i), (ii) and (iii), was to investigate whether or not the trend of settlements could be predicted for different twin tunnel configurations, i.e. when the stacked tunnels transitioned into a skewed configuration.

2.2.1 Method 1 - cavity expansion

A comprehensive explanation of the ground response curve developed using spherical and cylindrical expansion solutions for tunnel design has been detailed in Mair (2008). The ground movement is at the intersection between the line representing the tunnel lining support and the ground response curve (Figure 2).

An alternative approach of using cavity expansion solutions is to apply typical losses to the internal pressure acting on the excavation opening after the tunnel has advanced (Mair & Taylor, 1993).

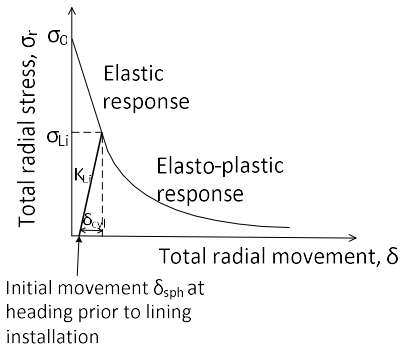

Figure 2 Illustration of ground response curve and lining response

2.2.2 Method 2 - Gaussian subsurface settlement profiles

Two methods were used in this study to predict the Gaussian subsurface settlement profile, namely (i) adopting a variation of settlement trough width with depth established in Mair et al. (1993) and (ii) using the solution proposed by Loganathan & Poulos (1998) which had been developed from the elastic solutions proposed by Verruijt & Booker (1996) and Sagaseta (1987).

By assuming that the volume losses at different depths are the same (equal-area method), the settlement trough width parameter, *i*, spanning a certain depth interval below the ground can be calculated from a pair of extensometer measurements. The derivation is shown in Appendix B.

2.2.3 Method 3- finite element analysis

The finite element method was also used to predict the displacements experienced by the upper tunnel. The finite element method is one of the routine means to obtain predictions in engineering practice. In this paper, a commercially available software, PLAXIS version 11, was used. The Soil Hardening model (Schanz et al., 1999) and drained analyses were adopted. In the model, the unloading stiffness was three times the loading stiffness and soil hardening followed a hyperbolic relationship. The performance of different soil models and different methods of modelling the volume loss were not investigated in this paper. Note that relevant discussions on some of the common methods to model volume loss induced by tunnelling can be found in Boon & Ooi (2016 a & b).

3. CHARACTERISTICS OF CASE HISTORY WITH FIELD MEASUREMENTS

Numerous tunnels have been constructed in Malaysia (Ha & Ooi, 2017; Ooi & Khoo, 2017). The case study is on the Sungai Buloh – Kajang (SBK) Line of the Klang Valley Mass Rapid Transit project in Kuala Lumpur which involved the construction of underground tunnels (Klados et al., 2015; Chin & Helliwell, 2015; Boon et al., 2015; Poh et al., 2014; Lim & Ng, 2015; Ooi & Ha, 2016 a) and underground stations (Tan et al., 2015; Boon et al., 2015b; Ooi & Ha, 2016 b). The inner and outer diameters of the tunnel rings are 5.8 m and 6.35 m respectively, and the thickness of the lining is 0.275 m (Poh et al., 2014). Each tunnel ring has a length of 1.4 m in the direction of the tunnel axis. The relevant tunnel alignment and ground profile in this chainage are shown in Figure 3 (a) and (b). In this chainage, the ground consists of the Kenny Hill Formation, which consists of quartzite and phyllite with a thick residual soil layer consisting of sandy silt and silty sand (Tan, 2017). The TBM shield length is approximately twice the TBM cutterhead diameter, and the distance between the two tunnels was approximately one diameter (1*D*) apart between their circumferences (see Figure 4).

(a)

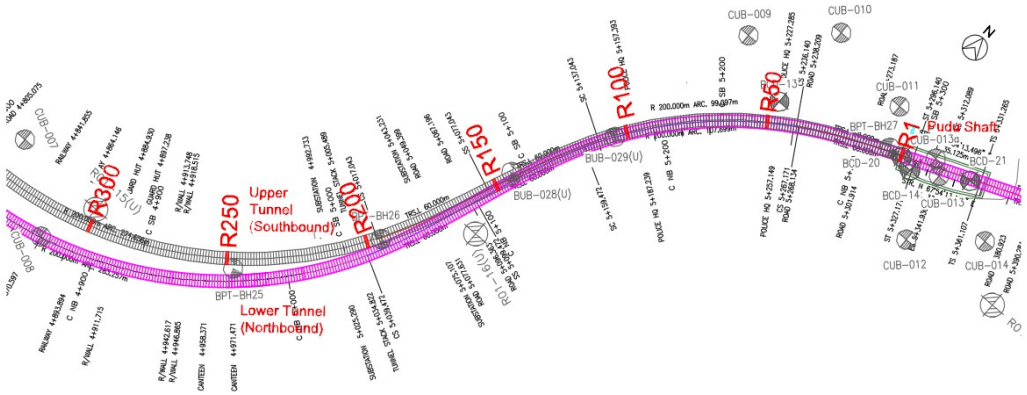

(b)

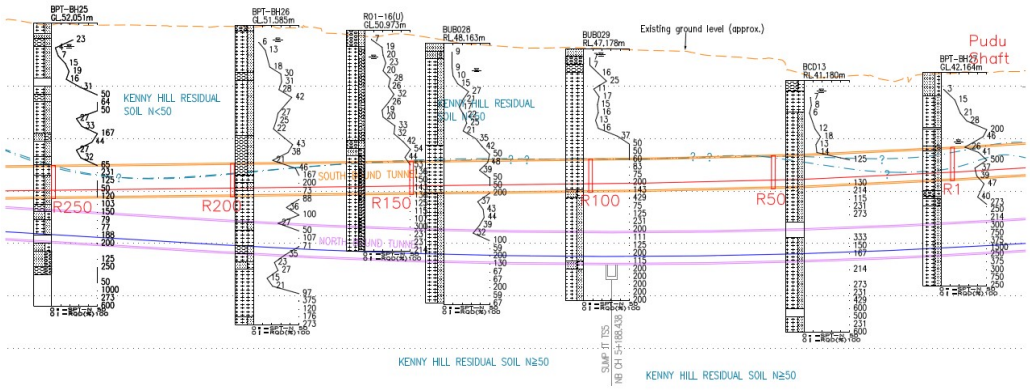

Figure 3 Stacked tunnel configuration: (a) plan view, (b) cross-sectional view for the plan view in (a)

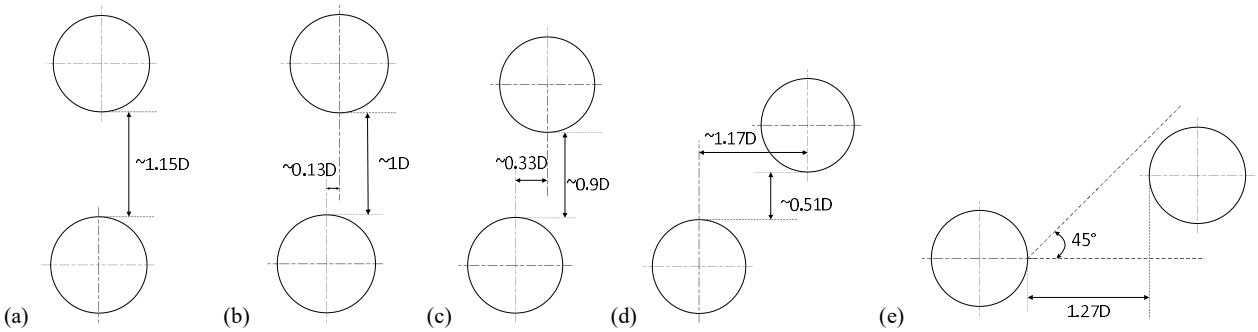

Figure 4 Position of upper tunnel with respect to lower tunnel for ring number (a) R40, (b) R120, (c) R160, (d) R215, (e) R300 Also see tunnel alignment in Figure 3.

The upper tunnel boring machine (TBM, earth pressure balance (EPB) machine) was launched from the launching shaft (Pudu Shaft in Figure 3 (a)) to construct the upper tunnel. However, the mine-through option was adopted at Pudu Shaft for the lower tunnel, and the same TBM (variable density machine in EPB mode) from an earlier chainage continued to mine through the shaft to optimise the construction programme. When the lower TBM arrived at Pudu Shaft, the upper tunnel had already been constructed, resulting in the sequence that the upper tunnel had to be subjected to undermining. The alignment of the twin tunnels was purely stacked for approximately the first 200 m.

The upper tunnel was monitored using four optical prisms, arranged as shown in Figure 5(a). The convergence was measured at every three rings. Furthermore, settlement markers were also installed to measure the precise levelling at every two tunnel rings. Figure 5 (a) shows a pair of settlement markers installed on a ring (for schematic convenience). Note, however, that only a piece of settlement marker was installed on any single ring on the alternating side of the invert. The settlements recorded consistently on the side closer to the lower tunnel were used for analysis.

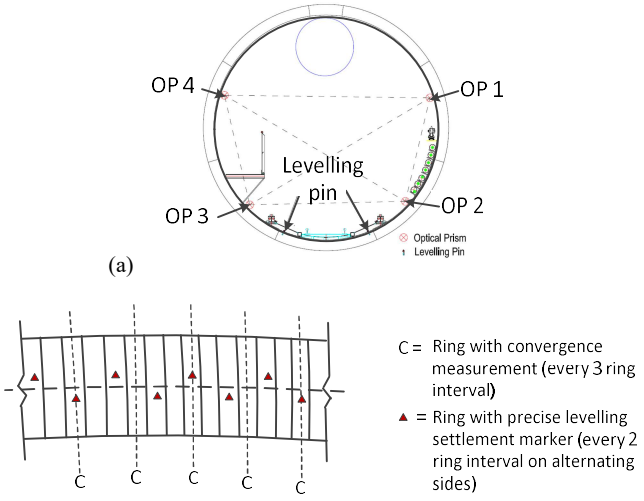

Figure 5 Monitoring programme consisting of optical prisms and settlement markers: (a) cross-section (along the tunnel drive), (b) layout plan of rings with convergence and precise levelling monitoring

Table 1 shows the parameters which had been adopted for this study as input to the Winkler beam analysis. References to the soil properties of the Kenny Hill Formation can be found in Wong & Muhinder (1996), Nithiaraj et al. (1996) and Kok (2006). A study was undertaken at a different chainage of the same Kenny Hill Formation in Kuala Lumpur to estimate the subsurface trough width using extensometer measurements at a greenfield area. The results appear to compare well with the empirical solution by Mair et al. (1993), as discussed in Appendix B, although this may not be completely representative of the entire Kenny Hill Formation as this measurement was made only at a localised area along the alignment.

Table 1 Parameters adopted for Winkler beam analysis

Parameters	Magnitudes
E_{lining}	32 GPa
$I_{cylinder}$	21 m^4/m
k_w	65.5 MN/m/m
E_{soil}	106 MPa, average SPT-N assumed as 53
v	0.25

4. RESULTS AND DISCUSSIONS

4.1 Longitudinal settlement profile for stacked conditions

The tunnel alignment (layout plan) had already been presented in Figure 3(a). The relative positions of both the upper and lower tunnel rings in a cross-sectional view are shown in Figure 4.

Figure 6 shows the measured settlements along the upper tunnel as the lower TBM mined underneath it. As the lower TBM advanced, more of the upper tunnel rings experienced settlements. Note that the TBM face shifts along the x-axis in Figure 6 as the TBM advances.

Figure 7 shows the deformations of the upper tunnel induced by the mining of the lower tunnel with reference to the lower TBM face, for the stretch of tunnel configurations which were purely stacked, i.e. until approximately R147. The figure was developed from measurements along the tunnel profile by using the lower TBM face as a reference point as the TBM mined underneath the upper tunnel. That is, Figure 7 shows the longitudinal settlement profile of the upper tunnel induced by undermining with x=0 being at the face of the lower TBM.

Figure 8 shows the settlements or heave experienced by a specific tunnel ring as the TBM mined past underneath it. This method of data presentation is different from Figure 7, because the displacements in Figure 8 are plotted at the same tunnel ring. A similar way of presenting the ground settlements could be found in Ilsley et al. (1991). Note that the ground condition related to these data points does not change since the same spot is measured (stationary measurement point).

The majority of the measurements of the settlement profiles were found to compare well with the Winkler beam solutions in Eq. (1) and (2) (see Figure 7 and Figure 8 (a)). Notice that the settlements in Figure 7 and Figure 8 (a) are normalised with respect to the final maximum settlement value, S_0, which can be estimated from the volume loss induced by tunnelling (Peck, 1969).

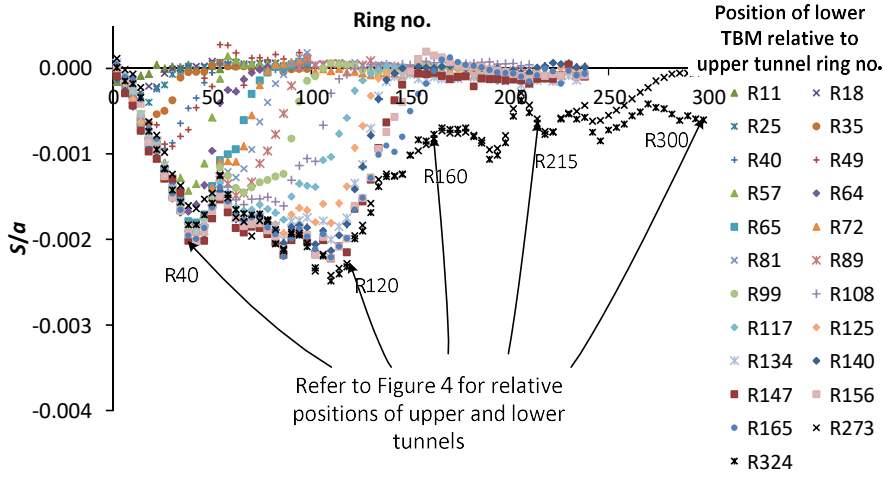

Figure 6 Measured upper tunnel settlement for different positions of the lower TBM cutterhead (in relation to upper tunnel ring)

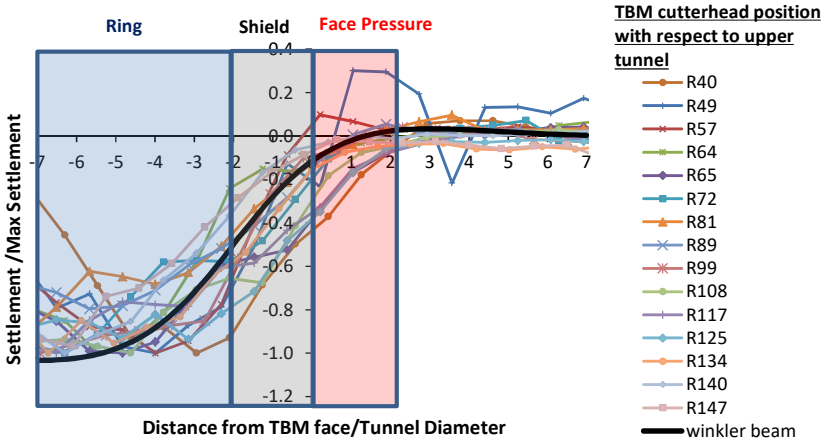

Figure 7 Longitudinal settlement profile of upper tunnel with respect to lower TBM face (different rings on the x-axis)

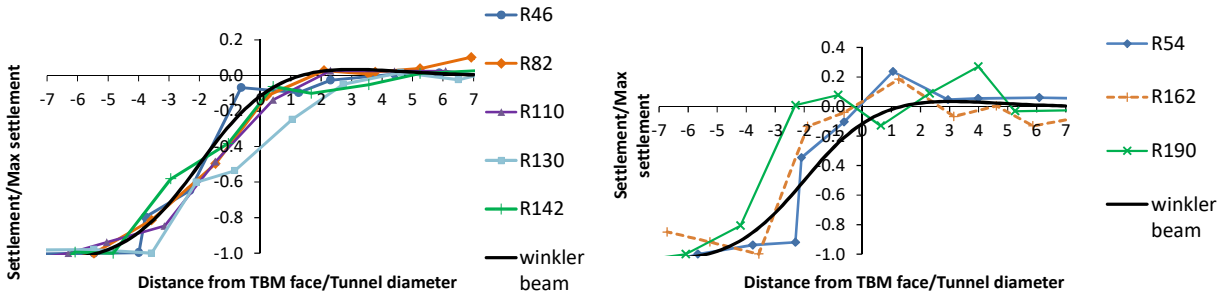

(a) (b)

Figure 8 Longitudinal settlement profile of upper tunnel developed by using a specific ring number as a reference point, and measuring the distance of the lower TBM face from it: (a) behaviour similar to a Winkler beam, and (b) heave at TBM face and abrupt settlement observed toward the TBM tail skin

The results in Figure 7 and Figure 8 show that 15% of the total settlements had taken place above the TBM face, 50% of total settlements had taken place behind the tunnel shield, and most of the settlements had taken place when the TBM face is 5*D* away. A schematic illustration is shown in Figure 9. This suggests that the influence of grouting between the annulus space between the shield and lining is important to control volume loss, as highlighted in Lee et al. (1992), Chou & Bobet (2002), and Thewes & Budach (2009). Further, it has been demonstrated in Boon et al. (2015 c) and Boon (2013) that, in addition to the hoop stiffness of the tunnel lining, the interface stiffness between the ground and the lining (related to the efficacy of annulus grouting) can affect the tunnel convergence. It is noted that the longitudinal displacement profile may be sensitive to the shield to tunnel diameter ratio (see also Thewes & Budach (2009) for comparison but for different shield length).

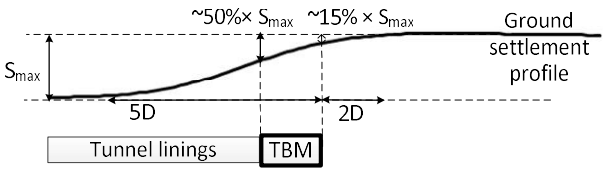

Figure 9 Schematic longitudinal settlement profile of upper tunnel with respect to shield TBM face from findings

In the more typical case, the tunnel ring settled in a more progressive manner (Figure 8 (a)). Nonetheless, it was observed that when the tunnel ring experienced upward heaving as the TBM face approached, the same tunnel ring was found to experience an abrupt settlement at the end of the TBM tailskin (Figure 8 (b)). There is no conclusive evidence explaining this finding, but may be due to several reasons, such as measurement accuracy or localised poorer soil conditions.

The influence of the launching shaft was non-negligible, acting as support to the tunnel rings. The results in Figure 6 presented previously show that the displacements closer to the launching shaft were small and gradually increased with the distance away from the shaft, after which the displacements tapered off when the influence of this boundary condition was negligible. A comparison between the field measurements and the predictions from the Winkler beam models (Eqs. (5) and (6)) is presented in Figure 10 (a), showing that the Winkler beam model with fixed-end boundary conditions obtained reasonable predictions.

It has to be cautioned that the Winkler beam solution presented in "normalised" displacements can yield counterintuitive results. Note that the slope of the longitudinal profile was ironically more gentle for lower subgrade stiffness values as shown in Figure 10 (a). The reason is that the solutions have been derived such that the far-ends of the beams experienced the same magnitude of far-field settlement asymptotically and this condition was met by indirectly adopting different "pressures", p, to satisfy $S_0 = p/k_w$ in the Winkler beam equation. For stiffer subgrades, the "pressures" (see Figure 1) were higher to meet the boundary conditions.

Instead of using a displacement based solution (to meet the far-end boundary condition of S_0), an alternative interpretation is to assume that there are actual pressure losses induced by the construction of the lower tunnel. This is more coherent with the conventional use of Winkler beam solutions, and the results are shown in Figure 10 (b). In this approach, a smaller subgrade stiffness value resulted in greater settlements, which is consistent with intuition.

Between the two approaches of using (i) normalised displacements and (ii) actual pressure losses, the approach of normalised displacements would be easier to use in engineering practice, as the maximum settlement can be calculated using well known relationships with tunnelling volume loss (Peck, 1969), whereas the estimation of pressure losses corresponding to a specified volume loss is more challenging.

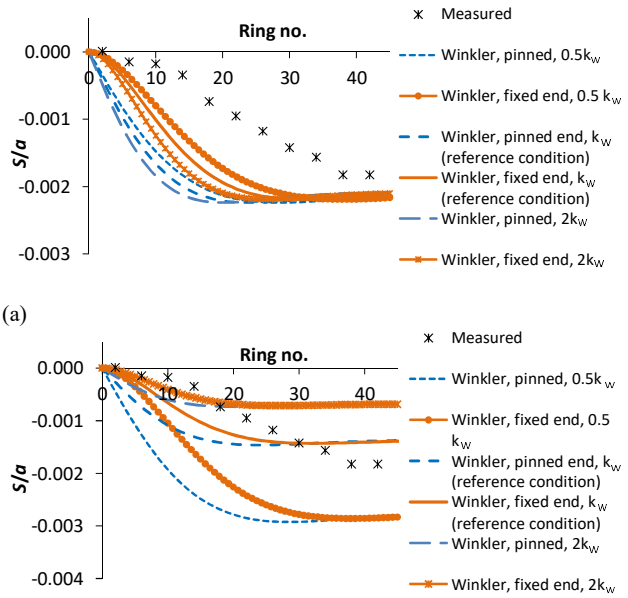

Figure 10 Measured and predicted displacements from Winkler solution based on fixed (solid lines) and pinned ends (dashed lines) for subgrade stiffness = k_w (reference condition), $2k_w$ and 0.5 k_w. Different plots:
(a) same final settlement plot and different pressures indirectly to satisfy $S_0 = p/k_w$ in Winkler beam theory, and
(b) plot with same magnitude of pressure loss (0.5 times p_0) but different final settlement values.

4.2 Transition from stacked to side-by-side

Recall the relative positions of the twin tunnels are shown in Figure 4. The interactions between the tunnels were studied using the methods discussed in Section 2. The results of cavity expansion solutions, subsurface Gaussian settlement solutions and finite element element analyses are presented here and compared with field measurements.

4.2.1 Precise levelling

As shown in Figure 6, the settlements experienced by the rings close to the launching shaft was negligible and increased gradually from R1 to R40, after which it tapered off at approximately S/a = 0.002. Then, from Ring 120 – 160 onwards, there was a declining trend in settlements, beyond which it tapered off at S/a = 0.0005. The results appear to indicate that the influence zone of the lower tunnel was limited to a narrow zone. The influence of undermining was minimal beginning from R160, at which the horizontal separation distance between the tunnel centres was merely 0.33*D* (Figure 4 (c)).

The results obtained from the ground response curves (concepts shown in Figure 2) are shown in Figure 11(a) (green crosses). The undrained shear strength was assumed to be 265 kPa, estimated as 5 times SPT-*N*. There are discrepancies between the field measurements and the predicted settlements with approximately 75% underprediction in terms of maximum values. This suggests that deformations due to face support and structural stiffness of the tunnel lining caused minimal stress-induced movement in the ground. This finding is somewhat in agreement with the earlier results of Figure 7 and Figure 9, where the settlement of the ring directly above the TBM face was only approximately 15% of the

total experienced settlements. This also highlights that other components of ground loss (apart from those due to stress changes of face pressure and tunnel stiffness) must be considered, such as overmining at the tunnel face, overcutting due to the design of the TBM cutterhead, and unfilled voids when grouting behind the tailskin, i.e. the gap between the tunnel rings and excavated opening (Kasper & Meschke, 2006).

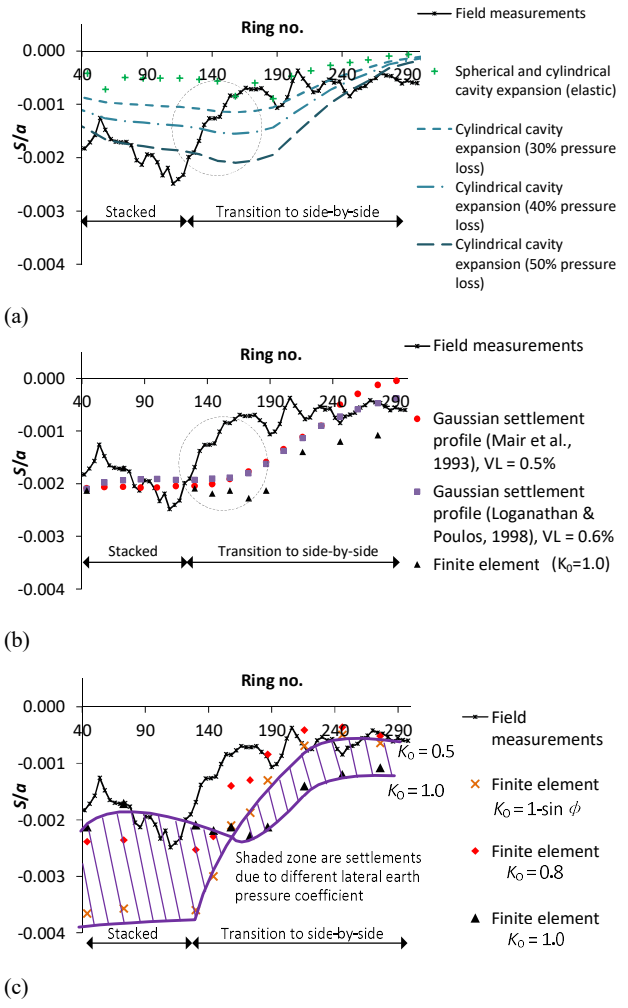

Figure 11 Predicted displacements obtained from
(a) cavity expansion solutions (displacements resolved in the vertical direction),
(b) sub-surface Gaussian settlement profiles,
(c) finite element analysis. Refer to Figure 4 for relative positions between tunnels

Solutions derived from cavity expansion based on the alternative approach of assuming a reduction in internal pressure (Mair & Taylor, 1993) were also used for comparison. For simplicity, the magnitude of pressure reduction was calculated here as a fraction of the overburden vertical pressure. The results of 30%, 40% and 50% of assumed pressure loss are plotted in Figure 11 (a) (blue dashed lines). The calculated settlement profiles obtained from the cavity expansion solutions experienced reduction in settlement magnitudes in a more gentle manner, when moving away from the stacked tunnel configuration, by comparison to the field measurements. The comparison suggests that greater reduction of internal pressure loss was required to match the field measurements when the tunnels were stacked directly, i.e. approximately 50% pressure loss by comparison to 30% pressure loss when the tunnels are side by side. The need for two different pressure losses to match the field measurements suggests that the stresses in the ground may not be isotropic.

The results of the two approaches to estimate the subsurface Gaussian settlement profile, i.e. Mair et al. (1993) and Loganathan & Poulos (1998) are shown in Figure 11 (b). Here, the magnitude of volume loss was calibrated when the tunnels were still purely stacked, and the same value was used to predict the settlements when they departed from the stacked configuration (see Figure 11 (b)). Note that a slightly larger magnitude of volume loss was used in the solution of Loganathan & Poulos (1998), i.e. 0.6%, compared with the solution of Mair et al. (1993), i.e. 0.5%, because the definitions of volume loss are different. The volume loss in Loganathan & Poulos (1998) refers to the material lost around the tunnel opening (the same magnitude may not be reflected on the ground surface), whereas the volume losses in the Peck (1969) and Mair et al. (1993) were derived from the surface settlements.

The trends obtained using the solutions proposed by Loganathan & Poulos (1998) and Mair et al. (1993) were very similar, as shown in Figure 11 (b). As the tunnels transitioned from a stacked into a skewed configuration, the predicted settlements decreased in a more gentle manner than the field measurements.

In the finite element analyses, four soil layers were adopted for analyses (see Figure 12) and the soil parameters are shown in Table 2. The axial and bending stiffness of the lining were assigned as 8.8 GPa/m and 18.100 MPa/m. The latter took into account of the reduction in bending stiffness due to the 7+1 tunnel segments forming a ring (Muir-Wood, 1975). A contraction of 1% (software function in PLAXIS to model volume loss) was adopted as the magnitudes of settlements compared well at the initial phase when the tunnels were purely stacked for K_0 =0.8 (red diamonds in Figure 11(c)).

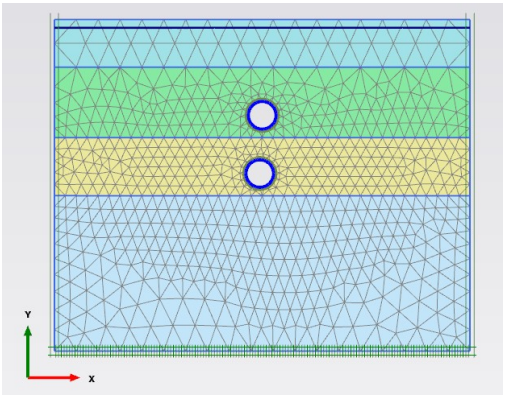

Figure 12 Set up of finite element analysis using the commercial software PLAXIS

Table 2 Soil parameters adopted for finite element

SPT	Unit weight, γ, (kN/m³)	Young's modulus, E_{50}' (MPa)	Cohesion, c' (kPa)	Friction angle, ϕ' (°)
14	18	24	5	28
53	19	92	10	28
120	20	209	15	29
200	20	250	15	38

The solutions obtained using the sub-surface Gaussian settlement profiles were found to compare well with finite element solutions (black triangles in Figure 11(b)) when the earth pressure coefficient at rest K_0 is 1.0, as shown in Figure 11 (b).

A general discussion of in-situ stresses in residual soils can be found in Vaughan et al. (1988). The influence of K_0 was investigated, and the results are shown in Figure 11 (c). For the two cases with K_0 < 1.0 (K_0 = 0.5 and 0.8), the settlement decreased more abruptly as the horizontal distance between the stacked tunnels increased. These results compare better with field measurements than the case with K_0=1.0. Note that, from R120 onwards (Figure 4 (b)), with the horizontal offset distance between the tunnel centres being approximately 0.13D, the settlements began to show signs of decrease. It was also found consistently that the impact of tunnel interaction was minimal starting from approximately R215 (Figure 4 (d)), with the horizontal offset distance between the tunnel centres being approximately 1.17D. For the case of K_0 = 0.5 (orange crosses in Figure 11 (c)) for the same magnitude of contraction in PLAXIS (to model volume loss), the settlements were greater (approximately 40% higher) when the tunnels were purely stacked initially, but the settlements began to converge to the magnitudes obtained using K_0=0.8 and 1.0 as the tunnels transitioned into a skewed configuration.

The reason for this abrupt decrease in settlement (dashed cricled region in Figure 11 (a) and (b)) as the horizontal distance between the tunnels increased was due to the compensating effects from the induced stresses in the ground. The ratio of minor to major principal stresses (σ_3/σ_1) are plotted in Figure 13 and the principal stress directions are plotted in Figure 14 using the boundary element software Examine 2D. The results that were obtained in Figure 13 may not provide the actual stress ratio, as the results were obtained for an unsupported opening in the ground, and the actual stresses may differ with the presence of internal support. However, they are adequate to demonstrate the influence of K_0. The results show that, for the case where K_0 < 1.0, the induced stress ratio (σ_3/σ_1) of a point "above" the tunnel opening is higher than the original stress ratio in the ground. On the other hand, the induced stress ratio (σ_3/σ_1) becomes lower than the original stress ratio as the point moves away horizontally from the tunnel (see Figure 13 (a)). The principal stress orientations are shown in Figure 14, where rotations of principal stresses are observed especially close to the opening. If the induced horizontal-to-vertical stress ratio (σ_h/σ_v) is lower than K_0, the ovalisation is of a pancake shape and is perpendicular to the ovalisation mechanism due to volume losses induced by tunnelling (see Figure 13 (a)). This compensating mechanism has contributed to a more abrupt change in trends. The larger magnitude of settlement for K_0 = 0.5 compared to the higher K_0 values obtained from finite element analyses is also due to the effects of induced stress ratio compounding with the deformations induced by volume loss. The influence of K_0 on tunnel deformation obtained from PLAXIS is shown in Figure 11 (c) as the shaded purple region, and is consistent with the findings obtained from boundary element analyses. A discussion of influence zones between adjacent excavation openings derived from elastic solutions are available in Bray (1986), and the discussion was based on changes in stress magnitudes of 5% from the original in-situ stresses. The analyses presented in Figure 13 are slightly different compared to Bray (1986), as Figure 13 aims to explain the ovalisation trends that were observed. It is noted that interactions between twin tunnels in a jointed rock mass are different, and discontinuum solutions are more appropriate (Boon et al., 2018).

Among the three methods of analysis, i.e. cavity expansion solutions, sub-surface Gaussian settlement profile method and finite element analysis, it was found that the finite element analyses gave the closest agreement to the trends observed in field measurements as it took into account of the in situ stresses. The decrease in settlements was most abrupt by comparison to other methods, as the tunnel moved away from the stacked configuration. Note that the actual settlement magnitudes obtained in the finite element analysis is a function of the magnitude of contraction and K_0. Therefore, underprediction and overprediction of settlement magnitudes due to K_0 cannot be interpreted in isolation of volume loss.

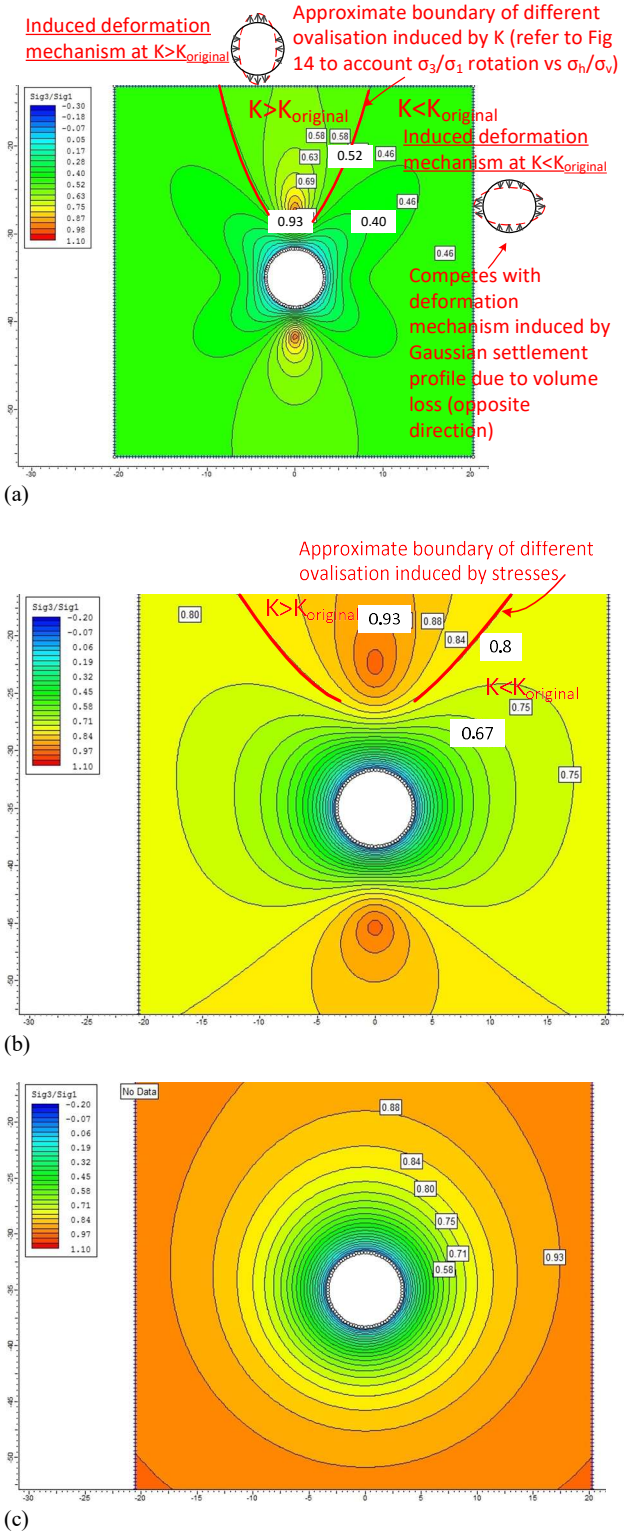

Figure 13 Contours of principal stress ratios from boundary element program (Examine 2D) and influence zone on deformation mechanisms for stress ratios: K_0 = (a) 0.5, (b) 0.8, (c) 1.0. The σ_3/σ_1 orientations have rotated from the original σ_h/σ_v especially close to the opening and have to be interpreted with Figure 14.

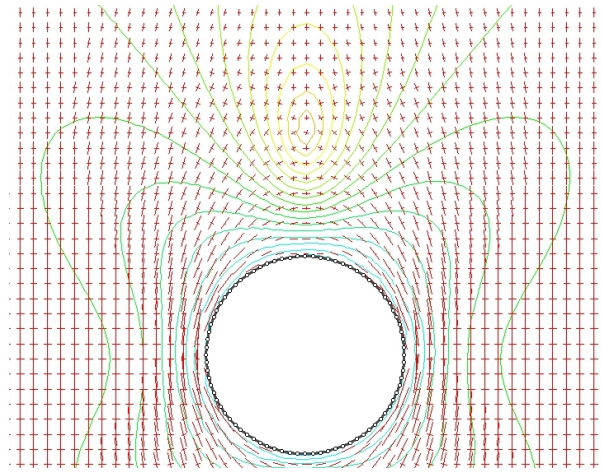

(a)

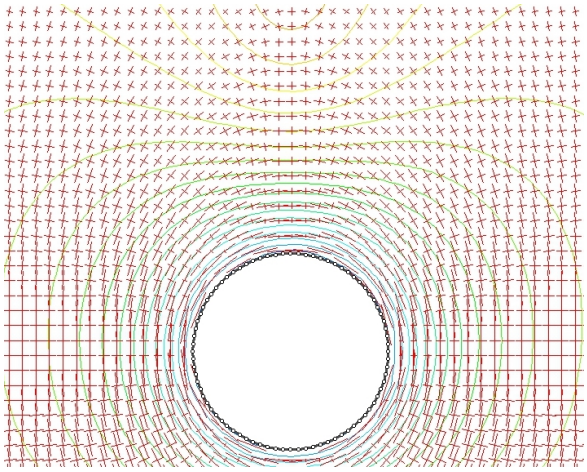

(b)

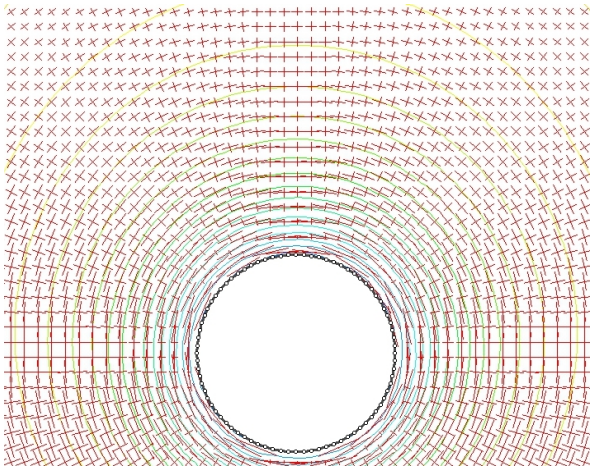

(c)

Figure 14 Principal stress directions (major and minor principal stresses) for stress ratios: K_0 = (a) 0.5, (b) 0.8, (c) 1.0

4.2.2 Convergence

The measured convergence in the vertical, horizontal and diagonal directions are shown in Figure 15 (a), (b) and (c) respectively (negative for shortening and positive for extension). The results indicate that the rings experienced extension in the vertical direction (Figure 15 (a)) at the beginning of the tunnel drive when they were stacked. The magnitude decreased gradually (shortened) as they departed from the stacked configuration at approximately Ring 120. Likewise, in the horizontal direction (Figure 15 (b)), there was shortening at the beginning and the magnitudes decreased as the tunnels departed from the stacked configuration. Both these observations suggest that the deformation mechanism was that of ovalisation. Comparisons with finite element analyses are also shown in the same figures. The change in sign of the convergence was more pronounced in the finite element analyses than the field measurements. The convergence measured in the diagonal directions suggests that the mechanism of ovalisation was skewed toward the lower tunnel, i.e OP 1 – 3 experienced extension whereas OP 2 – 4 experienced shortening.

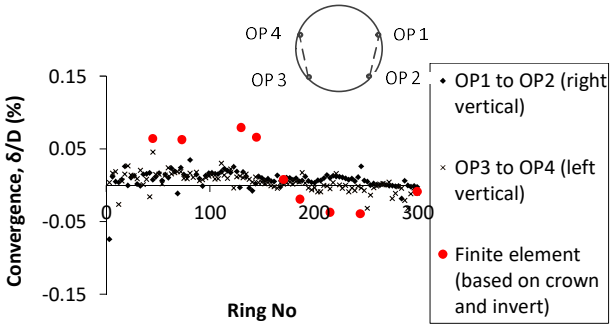

(a)

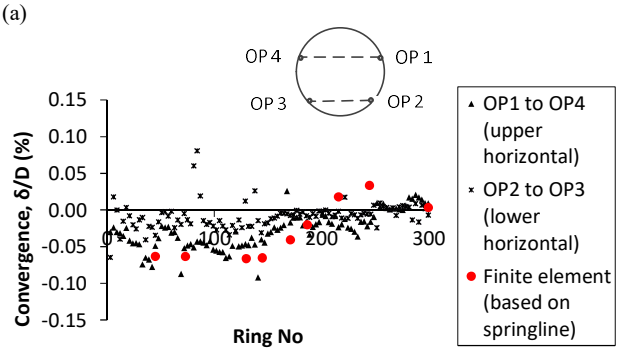

(b)

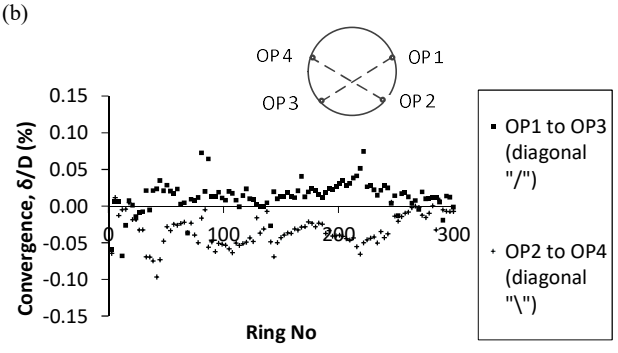

(c)

Figure 15 Measured convergence of upper tunnel due to impact of lower tunnel in the (a) vertical (OP1-OP2, OP3-OP4), (b) horizontal (OP1-OP4, OP2-OP3), and (c) diagonal direction (OP1-OP3, OP2-OP4), and comparison with finite element in (a) and (b). Positive for extension and negative for convergence.

4.2.3 Dimensionless charts of field measurements

In this Section, the field measurements are presented in terms of the relative positions between the twin tunnels in dimensionless form, normalised against the radius *a*. Figure 16 (a) shows the normalised settlement plotted against the normalised horizontal distance between the two tunnel centres. The results show that the impact of TBM undermining was dominant for horizontal distances less than 0.5*D* between the tunnel centres. Note that the edge-to-edge radial distance between the tunnels was approximately 1*D* apart throughout the plot in Figure 16. It was found that the horizontal distance between the tunnels had a dominating influence on the measured settlement by comparison to the vertical distance for this geometrical configuration (1*D* radial separation). Figure 16 (b) is another way of presenting the data, where the influence between two dimensionless groups is linear. Beyond a certain *a*/*h* value (Figure 16 b), when the two tunnels could be considered as purely stacked for practical purposes, the settlement magnitude reaches the limiting value. This graph is in contradiction to cavity expansion solutions used to study soil movement in Londay Clay (overly consolidated), in which the displacements increase with *a*/*r* (Mair & Taylor, 1993), implying that the displacements should be roughly constant due to similar radial offset distance between the tunnel centres. It is reminded that in Mair & Taylor (1993), although cavity expansion solutions based on isotropic stress conditions were used to study soil movement due to tunnelling, the field measurement for vertical soil movement above the tunnel and horizontal soil movement at the level of the tunnel was plotted into two distinct lines (Mair & Taylor, 1993), implying anisotropy in terms of ground movement.

The trend in Figure 16 is believed to be affected by the in-situ stresses. It is noted that the influence zone for tunnel-tunnel interactions could be different from tunnel-pile interactions as a pile body extends all the way from the ground surface till the pile toe and is more influenced by the soil settlement trends along the pile (Boon & Ooi, 2016 a).

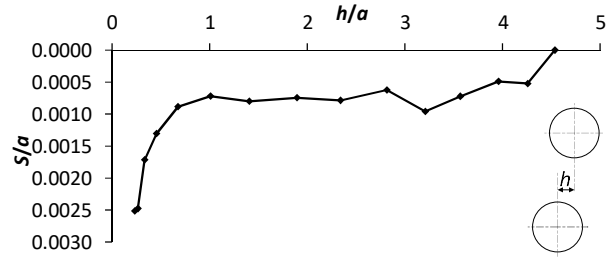

(a)

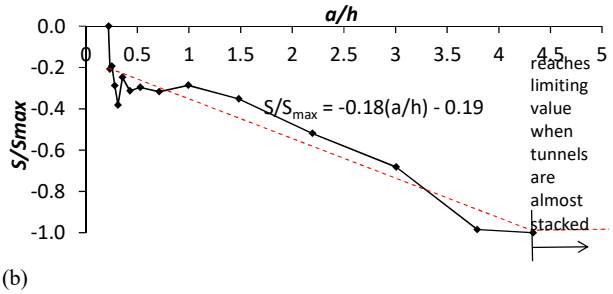

(b)

Figure 16 Decline in settlement of upper tunnel as horizontal distance between the tunnels increases where the x-axis is (a) *h*/*a* and (b) *a*/*h*. Edges of tunnels are radially apart by approximately 1*D* distance

4.2.4 Construction with lower tunnel first

The impact of the second tunnel onto the first tunnel is compared between (i) the case where the upper tunnel was constructed first and (ii) the case where the lower tunnel was constructed first. The finite element results indicate that the magnitudes of settlement and convergence (Figure 17 (a), (b) and (c)) are more than five times larger when the top tunnel was constructed first (magnitude difference between red circles and blue diamonds). This highlights the importance of thorough analytical and numerical analyses for this unconventional tunnelling sequence. The finding is consistent with Addenbrooke & Potts (2001), where the movement was more than 4 times between the two sequences, for the case where the edge-to-edge separation distance between the lining was approximately its tunnel diameter. The impact is smaller if the bottom tunnel is constructed first because the impact of volume loss to an object below the tunnel is negligible. The observation that the sign of convergence for the two cases (upper tunnel or lower tunnel first, blue diamonds and red circles in Figure 17 (b)) are different is counterintuitive because the lower tunnel would be expected to ovalise into an egg shape when there is relief of overburden pressure due to the excavation of the upper tunnel.

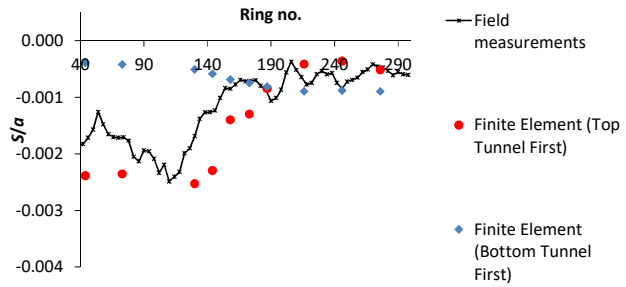

(a)

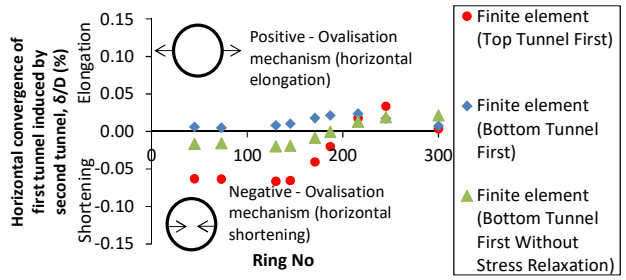

(b)

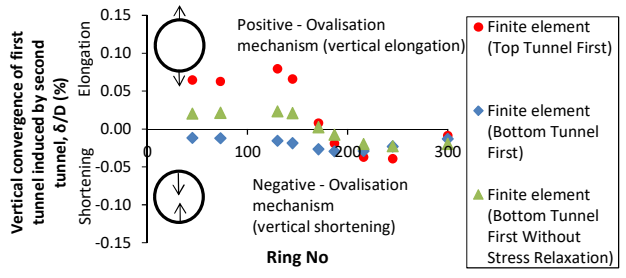

(c)

Figure 17 Comparison between two tunnel construction sequences: (a) precise levelling, (b) horizontal convergence and (c) vertical convergence of first tunnel induced by construction of second tunnel

The counterintuitive ovalisation pattern into a pancake shape (blue diamonds in Figure 17 (b) and (c)) was found to be due to the modelling of volume loss of the first tunnel. When no stress relaxation was allowed (due to contraction or volume loss), the ovalisation shapes were the same for both cases but with different magnitudes (red circles and green triangles in Figure 17(b)). With stress relaxation (see Figure 14 for extreme case of unsupported opening), the creation of a new neighbouring opening may increase the ground stresses (relative to the relaxed ground) and induce a pancake shape deformation onto the first tunnel. This observation has been verified using the alternative internal pressure method of modelling volume losses in finite element analyses (refer to Boon & Ooi, 2016 a), and the same trends were obtained.

5. CONCLUSIONS

In terms of theoretical development, original insight was obtained with regard to the construction of stacked twin tunnels, with the upper tunnel constructed first and subsequently undermined by the lower tunnel. The analyses presented here revealed the important parameters affecting the response of an existing tunnel due to undermining by shield tunnelling and the limitations of common solutions used to study soil movements induced by a single tunnel. It is shown that the longitudinal settlement profile of the upper tunnel could be analysed as a Winkler beam. The Winkler beam analyses, with the assumption of loss of support pressure behind the TBM shield, resulted in good agreement with field measurements with regard to the deflected shape of the upper tunnel (settlements normalised by maximum settlement) at different points of interests with respect to the lower TBM face.

The influence of the launching shaft was found to be non-negligible. This could also be analysed using the Winkler beam framework by assigning fixed end boundary conditions at the far-end connected to the launching shaft as a first approximation.

To predict the magnitudes and trends of settlements as the tunnels departed from the stacked configuration, several methods were explored, namely (i) cavity expansion solutions, (ii) the method of sub-surface Gaussian settlement profile based on the approaches proposed by Mair et al. (1993) and Loganathan & Poulos (1998), as well as (iii) the finite element method. Note that an "equal area method" using extensometer measurements to estimate the sub-surface trough width parameter, i, is presented in Appendix B. The estimated trough width parameters were obtained at localised areas only and may not be representative of the entire geological formation.

The influence of in-situ stresses K_0 was found to be important. Finite element analyses and cavity expansion solutions assuming isotropic stresses, as well as solutions calculating the subsurface Gaussian settlement profile, predicted a gentler decline in settlements by comparison to field measurements as the horizontal distance between the stacked tunnels increased.

Finite element analysis with K_0 less than 1.0, which is consistent with the case of residual soils, gave better predictions of the tunnel deformation trends. The predicted reduction in settlements as the tunnels deviated from the stacked configuration was more abrupt and was consistent with field measurements.

The field measurements were presented in two dimensionless charts, which could be relevant for residual soils with horizontal earth pressure coefficient lower than 1.0 and edge-to-edge distance of one tunnel diameter between twin tunnels. The first chart (Figure 7) shows the longitudinal settlement profile for the chainage where the tunnels were purely stacked, but may be influenced by the TBM shield length to diameter ratio. The second chart (Figure 16) shows the decline in impact as the tunnels began to depart from the stacked configuration. The latter was found to follow an inverse relationship with the settlements experienced by the upper tunnel. These findings could assist in the development of monitoring programme in construction. For instance, using a 45° line (Figure 4(e)) to establish the influence zone may be conservative, since tunnel interaction was negligible when the horizontal offset distance between the tunnel centres was 1D apart in the Kenny Hill Formation. For conservatism, the monitoring zone could be extended, while varying the spatial intensity of monitoring based on the anticipated magnitudes of settlements. The information that 15% of the maximum settlement would have had taken place above the TBM face, approximately 50% of the maximum settlement would have had taken place at the TBM tailskin, and most of the settlement would have had taken place 5D away from the TBM cutterhead could also assist in the development of the spatial intensity of monitoring. By considering also the rate of TBM mining per day, the measurement points could be spaced so that adequate reaction time is possible.

The situation of undermining a pre-existing tunnel in a longitudinal direction is uncommon but can arise since there is increasing use of underground space in urban areas. This situation can also arise due to a change in construction programme in order to interface with the progress of station excavations for a metro project. The analyses and discussions in this paper set out a useful framework to analyse one of the problems which could be encountered in tunnelling and underground metro projects, and more specifically to check against tolerance requirements in segmental lining design or track design (The British Tunnelling Society & The Institution of Civil Engineers, 2010) to evaluate the need and extent of protective measures if required.

6. ACKNOWLEDGEMENTS

Thanks are due to Mr. B.H. Pua, Mr. A. Zaifliqhar, Ms. Y. Y. Low, Mr. X.Z. Tung, Mr. Vasagavijayan S., Ir. J.G. Tan, Mr. Ramesh K., Mr. Izlan S., who had assisted in the management of data acquisition and monitoring.

7. APPENDIX A: DERIVATION OF WINKLER BEAM WITH END SUPPORTS: FIXED AND PINNED

The general solution of a Winkler beam solution with end supports can be expressed as (Den Hartog, 1952):

$$y = e^{-\beta x}\left(A\cos\beta x + B\sin\beta x\right) - \frac{p_0}{k} \quad \text{(A1)}$$

The term $-p_0/k$ could be substituted with S_0, which is the negative displacement experienced at the far end, such that:

$$y = e^{-\beta x}\left(A\cos\beta x + B\sin\beta x\right) + S_0 \quad \text{(A2)}$$

With support at one end (fixed or pinned), one of the boundary conditions is that x=0 and y=0, from which we can infer that A =-S_0. For fixed end support, the boundary condition is x=0 and y'=0, which leads to:

$$y' = \beta e^{-\beta x}\left((S_0 + B)\cos\beta x + (S_0 - B)\sin\beta x\right) \quad \text{(A3)}$$

from which we obtain B = -S_0. Finally, we obtain:

$$y = S_0\left(1 - e^{-\beta x}\left(\cos\beta x + \sin\beta x\right)\right)$$

For pinned end support, the boundary condition is x=0 and y''= 0, from which we can infer that the constant B = 0. For this, we obtain:

$$y = S_0\left(1 - e^{-\beta x}\cos\beta x\right) \quad \text{(A5)}$$

The derivation above are analytically straightforward. It is noted that attempts to predict induced displacements due to excavations above tunnels with different longitudinal extents and with the influence of boundary conditions were presented in Boon et al. (2016), making use of solutions for differential equations with respect to (x/a) in Flügge (1973) and analogies with the Winkler beam theory.

8. APPENDIX B: COMPARISON OF K FOR SUB-SURFACE GAUSSIAN SETTLEMENTS BASED ON EXTENSOMETER MEASUREMENTS

By assuming that the volume losses (area of the sub-surface settlement profiles) at different depths are the same (see Figure B1), it is possible to derive the parameter k governing the settlement trough width of the soil at a certain depth interval from a pair of extensometer readings.

Take the subsurface settlement profile, S_1, at a vertical distance z_1 from the tunnel centre as:

$$S_1 = S_{\max 1} e\left(\frac{-y_1^2}{2i_1^2}\right) \tag{B1}$$

where y_1 is the horizontal distance from the tunnel axis, i_1 as the point of inflection, and S_{max1} as the settlement above the tunnel crown. Similarly the subsurface settlement profile at the vertical distance z_2 from the tunnel centre is expressed here as:

$$S_2 = S_{\max 2} e\left(\frac{-y_2^2}{2i_2^2}\right) \tag{B2}$$

From Eq. (B1) and (B2), we obtain:

$$\frac{S_1}{S_2} = \frac{S_{\max 1}}{S_{\max 2}} e\left(\frac{-y_1^2}{2i_1^2} + \frac{y_2^2}{2i_2^2}\right) \tag{B3}$$

The volume loss can be expressed as:

$$V_{s1} = \sqrt{2\pi} i_1 S_{\max 1} \tag{B4}$$

and

$$V_{s2} = \sqrt{2\pi} i_2 S_{\max 2} \tag{B5}$$

Assuming that the volume loss at different depths are the same, we equate (B4) and (B5) such that:

$$\sqrt{2\pi} i_1 S_{\max 1} = \sqrt{2\pi} i_2 S_{\max 2} \tag{B6}$$

With $i=kz$, and assuming that the k values in between depth z_1 and z_2 are the same, we obtain:

$$\frac{S_{\max 1}}{S_{\max 2}} = \frac{z_2}{z_1} \tag{B7}$$

Substituting (B7) into (B3):

$$\frac{S_1}{S_2} = \frac{z_2}{z_1} e\left(\frac{-y_1^2}{2k^2 z_1^2} + \frac{y_2^2}{2k^2 z_2^2}\right) \tag{B8}$$

Eq. (B8) can be further expressed as:

$$\ln \frac{S_1 z_1}{S_2 z_2} = \frac{1}{2k^2}\left(\frac{-y_1^2}{z_1^2} + \frac{y_2^2}{z_2^2}\right) \tag{B9}$$

and finally as:

$$k = \sqrt{\frac{\left(\frac{-y_1^2}{z_1^2} + \frac{y_2^2}{z_2^2}\right)}{2\ln \frac{S_1 z_1}{S_2 z_2}}} \tag{B10}$$

Note that the magnitudes of S_1 and S_2 could be obtained from extensometers.

The surface settlement profiles induced by tunnelling across two cross-sections which are sited in greenfield conditions are shown in Figure B2.

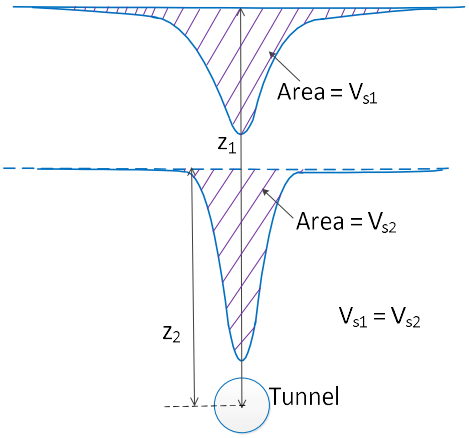

Figure B1 Assumption of equal volume losses at different depths

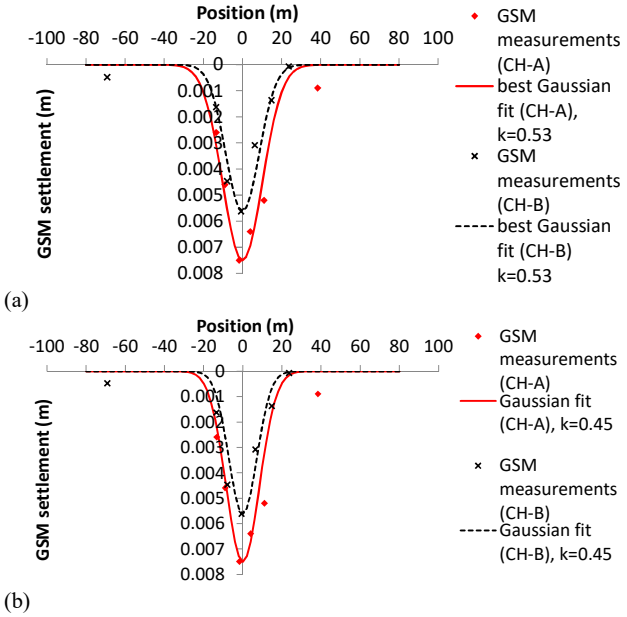

Figure B2 Surface settlement profiles and the fitting of Gaussian functions: (a) best fit using least squares, (b) adopted in the project. CH-A. Tunnel centre of CH-A is 18.9 m bgl and tunnel centre of CH-B is 16 m bgl.

The Greenfield sites are located at another chainage with the same geological formation. The best fit k value is obtained as 0.53; this value does not vary too much from the magnitude of 0.45 adopted for the project. The k-values at different depths were calculated using Eq. (B10) from different combinations of extensometer readings (see Figure B3). The calculation was carried out on the (i) same rod extensometers only, and (ii) between different rod extensometers at the same chainage. Only the closest pairs of depth combinations were used in the study, to avoid taking overly large depth intervals when estimating the k value. The results are shown in Figure B4.

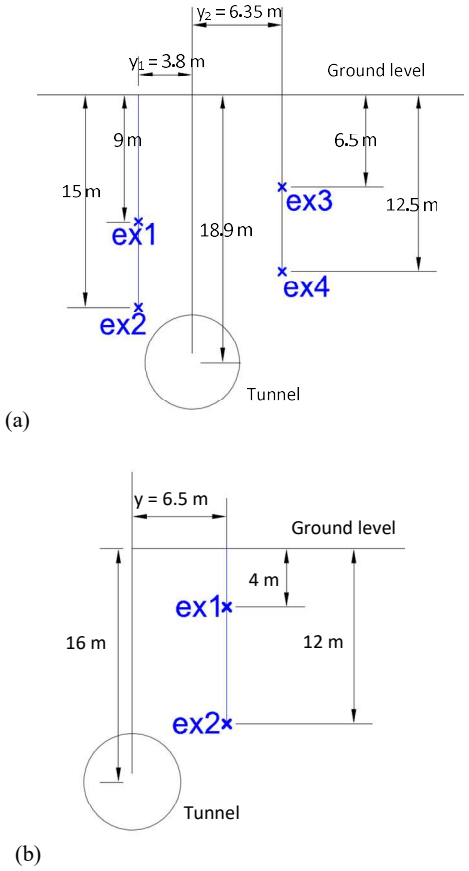

Figure B3 Extensometers (EXs) installed next to tunnel (diameter = 6.67 m) in (a) CH-A and (b) CH-B

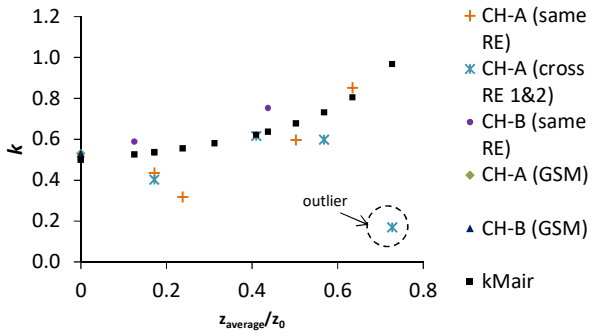

Figure B4 Calculation of k values: from readings obtained from (i) the same rod extensometer, (ii) from different rod extensometers, and (iii) from ground settlement markers (Figure B3). The results are compared with the empirical solution of Mair et al. (1993)

The derived k values are compared with the empirical solution from Mair et al. (1993):

$$k = \frac{0.175 + 0.325\left(1 - \frac{z_g}{z_0}\right)}{1 - \frac{z_g}{z_0}} \qquad \text{(B11)}$$

from which, the point of inflection i is obtained as:

$$i = kz \qquad \text{(B12)}$$

where z_g is the depth below the ground surface, z is the vertical distance above the tunnel centre, and z_0 is the depth of tunnel axis level.

The derived subsurface k values compare well with Eq. (B11) (Mair et al., 1993) as shown in Figure B4, apart from the pair of extensometer closest to the tunnel (located at a vertical distance of approximately 0.1D and 0.5D from the tunnel crown). This might be due to the chimney-like mechanism reported by Marshall et al. (2012), Potts (1976) and Cording (1991), which relates to a smaller k value. Note that the presented results are for localised locations and may not be representative of the entire geological formation.

9. REFERENCES

Addenbrooke, T.I. and Potts, D. M. (2001). "Twin tunnel interactions: surface and subsurface effects". The International Journal of Geomechanics, 1(2), 249-271.

Afifipour, M., Sharifzadeh, M., Shahriar, and K. Jamshidi, H. (2011). "Interaction of twin tunnels and shallow foundation at Zand underpass", Shiraz metro, Iran. Tunnelling and Underground Space Technology, 26, 356-363.

Bobet, A. (2001). "Analytical solutions for shallow tunnels in saturated ground". J. Eng. Mech. –ASCE, 127(12), 1258-1266.

Boon, C.W (2013). "Distinct element modelling of jointed rock masses: algorithms and their verification". D.Phil. thesis, University of Oxford.

Boon, C. W., Teh, E.H., and Ooi, L.H (2015a). "Protection of buildings and structures within the influence of tunnelling works". International Conference and Exhibition on Tunnelling & Underground Space (ICETUS 2015), 3 – 5 March, Ooi T.A., Ooi, L.H. (Eds.), Tunnelling & Underground Space Division, The Institution of Engineers, Malaysia, 256-262.

Boon, C.W., Ooi, L.H., and Low, Y.Y. (2015b). "Performance of ground anchors in a Mass Rapid Transit project in Malaysia". 9th International Symposium on Field Measurements in Geomechanics (FMGM), 9-11 September, Dight, P. (Eds.), Sydney, Australia, Australian Centre for Geomechanics, 621-630.

Boon, C.W., Houlsby, G.T., and Utili, S. (2015c). "Designing tunnel support in jointed rock masses via the DEM". Rock Mechanics and Rock Engineering, 48, 603-632.

Boon, C.W. and Ooi L.H. (2016a). "Tunnelling Past Critical Structures in Kuala Lumpur: Insights from Finite Element Analysis and T-Z Load Transfer Analyses". Geotechnical Engineering Journal of the SEAGS & AGSSEA, Vol. 47, No.4, pp 109-122.

Boon, C.W. and Ooi, L.H. (2016b). "Type II Factor of Safety: Reliability of Information from Instrumentation, Numerical Analysis, Site Investigation and Design", 19th Southeast Asian Geotechnical Conference & 2nd AGSSEA Conference (19SEAGC & 2AGSSEA) Young Geotechnical Engineers Conference, The Institution of Engineers Malaysia, pp 53-58.

Boon, C.W., Ooi, L.H., Tan, J.G., and Low, Y.Y. (2016). "Geotechnical considerations of deep excavation design for TBM bore-through with a case history in Kuala Lumpur",

Geotechnics for Sustainable Infrastructure Development, Geotec Hanoi 2016, pp 375-384.

Boon, C.W., Neo, C.W., Ng, D.C.C., and Ong, V.C.W. (2018). "Discontinuum analyses of openings constructed with side drift and limited rock cover". J Zhejiang Univ-Sci A (Appl Phys & Eng), 19(4), 255-265.

Bray, J.W. (1986). "Chapter 2: Some Applications of Elastic Theory. Analytical and Computational Methods in Engineering Rock Mechanics." Analytical and Computational Methods in Engineering Rock Mechanics (Brown E.T. Eds.), Allen & Unwin, London.

Boonyarak, T. and Ng, C.W.W. (2015). "Effects of construction sequence and cover depth on crossing-tunnel interaction". Canadian Geotechnical Journal, 52, 851-867.

Burd, H.J., Houlsby, G.T, Augarde, C.E, and Liu, G, (2000). "Modelling Tunnelling-Induced Settlement of Masonry Buildings". Proc. ICE, Geotechnical Engineering, 143, 17-29.

Chakeri, H., Hasanpour, R., Hindistan, M. A., and Unver, B. (2011). "Analysis of interaction between tunnels in soft ground by 3D numerical modelling". Bull Eng Geol Environ, 70, 439-448.

Chen, R.P., Zhu, J., Liu, W., and Tang, X.W. (2011). "Ground movement induced by parallel EPB tunnels in silty soils". Tunnelling and Underground Space Technology, 26, 163-171.

Chin, R. M. and Heliwell, D.M., (2015). "Performance of EPB Tunnelling in Kenny Hill". International Conference and Exhibition on Tunnelling & Underground Space (ICETUS 2015), 3 – 5 March, Ooi T.A., Ooi, L.H. (Eds.), Tunnelling & Underground Space Division, The Institution of Engineers, Malaysia, 298-301.

Chou, W.-I., and Bobet, A., (2002). "Predictions of ground deformations in shallow tunnels in clay". Tunnelling and Underground Space Technology, 17, 3-19.

Chu, B.-L., Hsu, S.-C., Chang, Y.-L., and Lin, Y.-S., (2007). "Mechanical behaviour of a twin-tunnel in multi-layered formations". Tunnelling and Underground Space Technology, 22, 351-362.

Cording, E. J., (1991). "Control of ground movements around tunnels in soil". Proc. 9th Pan-American Conf. Soil Mech. Found. Engng, Valparaiso, 2195-2244.

Den Hartog, J. P., (1952). "Advanced strength of materials". McGraw-Hill. Dover Edition 1987, 1-378.

Do, N.-A., Dias, D., Oreste, P., and Djeran-Maigre, I., (2014). "Three-dimensional numerical simulation of a mechanized twin tunnels in soft-ground". Tunnelling and Underground Space Technology, 42, 40-51.

Fang, Q., Zhang, D., Li, Q. and Wong, L. N. Y., (2015). "Effects of twin tunnels construction beneath existing shield-driven twin tunnels". Tunnelling and Underground Space Technology, 45, 128-137.

Fang, Q., Tai, Q., Zhang, D., and Wong, L.N.Y. (2015). "Ground surface settlements due to construction of closely-spaced twin tunnels with different geometric arrangements". Tunnelling and Underground Space Technology, 51, 144-151.

Flűgge, W. (1973). Stresses in Shells. Springer-Verlag New York Heidelberg Berlin, 2nd Ed., pp 525.

Franza, A., Haji, T. K., Marshall, A.M. (2016). "A winkler-based method for the assessment of tunnelling induced deformations on piled structures". Geo-China 2016, GSP 260, pp 259-260.

Ha, T. T. and Ooi, L. H. (2016). "Positioning to undertake underground works contracts – a Malaysian experience". Southeast Asian Conference and Exhibition in Tunnelling and Underground Space 2017 (SEACETUS 2017), Subang Jaya, Malaysia, 18-19 April 2017, pp 39-50.

Hage Chehade, F. and Shahrour, I., (2008). "Numerical analysis of the interaction between twin tunnels: Influence of the relative position and construction procedure". Tunnelling and Underground Space Technology, 23, 210-214.

Ilsley, R. C., Hunt, S. H., Komurka, V.E., Doyle, B. R., and Ramage, J., (1991). "Ground movements around tunnels excavated in Milwaukee, USA, using slurry shield and earth pressure balance methods". Proceedings of the 4th International Conference on Ground Movements and Structures, Session VII, 714-738.

Kasper, T. and Meschke, G., (2006). "On the influence of face pressure, grouting pressure and TBM design in soft ground tunnelling". Tunnelling and Underground Space Technology, 21, 160-171.

Klados, G., Ng, H.W., Wong, G.C.Y., and Chin, J.H.H., (2015). "Managing tunnelling challenges through Kuala Lumpur karst formation using variable density TBMs". International Conference and Exhibition on Tunnelling & Underground Space (ICETUS 2015), 3 – 5 March, Ooi T.A., Ooi, L.H. (Eds.), Tunnelling & Underground Space Division, The Institution of Engineers, Malaysia, 186-191.

Klar, A., Vorster, T.E.B., Soga, K., Mair, R. J., (2005). "Soil-pipe interaction due to tunnelling: comparison between Winkler and elastic continuum solutions". Géotechnique, 55 (6), 461-466.

Kok, Y. L., (2006). "Investigating the mechanical behaviour of two residual soils from Malaysia". Ph.D. thesis. University of Cambridge. 1-309.

Kouretzis, G. P., Karamitros, K. D., and Sloan, S.W., (2015). "Analysis of buried pipelines subjected to ground surface settlement and heave", Canadian Geotechnical Journal, 52, 1058-1071.

Law, K.H., Hashim, R., and Ismail, Z. (2013). "Performance of multi-propped deep excavation in Kenny Hill Formation". Advances in Geotechnical Infrastructure. Leung, C.F., Goh, S.H., Shen, R.F. (Eds.), Geotechnical Society of Singapore, 705-712.

Lee, R.G., Rowe, R.K., and Lo, K.Y., (1992). "Subsidence owing to tunnelling I: Estimating the gap parameter". Canadian Geotechnical Journal, 29, 929-940.

Li, X. G., and Yuan, D. J., (2012). "Response of a double-decked metro tunnel to shield driving of twin closely under-crossing tunnels". Tunnelling and Underground Space Technology, 28, 18-30.

Lim, H.Y. and Ng, H.W., (2015). "Steel Fibre Reinforced Concrete Tunnel Lining Segments". International Conference and Exhibition on Tunnelling & Underground Space (ICETUS 2015), 3 – 5 March, Ooi T.A., Ooi, L.H. (Eds.), Tunnelling & Underground Space Division, The Institution of Engineers, Malaysia, 198-207.

Liu, H. Y., Small, J. C. and Carter, J. P., (2008). "Full 3D modelling for effects of tunnelling on existing support systems in the Sydney region". Tunnelling and Underground Space Technology, 23, 399-420.

Liu, H. Y., Small, J. C., Carter, J. P., and Williams, D. J. (2009). "Effects of tunnelling on existing support systems of perpendicularly crossing tunnels". Computers & Geotechnics, 36, 880-894.

Liu, H., Li, P. and Liu, J. (2011). "Numerical investigation of underlying tunnel heave during a new tunnel construction". Tunnelling and Underground Space Technology, 26, 276-283.

Loganathan, N. and Poulos, H.G. (1998). "Analytical prediction for tunneling-induced ground movements in clays". J. Geotech. and Geoenvir. Eng. 124(9), 846-856.

Loganathan, N. (2011). "An innovative method for assessing tunnelling-induced risks". Parsons Brinckerhoff 2009 William Barclay Parsons Fellowship Monograph 25. First Printing 2011, New York.

Mair, R.J., Taylor R.N., and Bracegirdle, A. (1993). "Subsurface settlement profiles above tunnels in clays". Géotechnique 43(2), 315-320.

Mair, R. J. (2008). "Tunnelling and geotechnics: new horizons". Géotechnique 58(9), 695-736.

Mair, R.J. and Taylor, R.N., (1993). "Prediction of clay behaviour around tunnels using plasticity solutions". Predictive Soil Mechanics: Proceeedings of the Wroth Memorial Symposium, Oxford, 27-29 July 1992, Thomas Telford London, 449-463.

Marshall, A. M., Klar, A., and Mair, R. J. (2010). "Tunneling beneath buried pipes: view of soil strain and its effect on pipeline behaviour". Journal of Geotechnical and Geoenvironmental Engineering, 136 (12), 1664-1672.

Marshall, A. M., Farrell, R., Klar, A., and Mair, R. J., (2013). "Tunnels in sands: the effect of size, depth and volume loss on greenfield displacements". Géotechnique, 62 (5), 385-399.

Mirhabibi, A. and Soroush, A. (2012). "Effects of surface buildings on twin tunnelling-induced ground settlements". Tunnelling and Underground Space Technology, 29, 40-51.

Mohamad, H., Bennett, P. J., Soga, K., Mair, R. J., and Bowers, K., (2010). "Behaviour of an old masonry tunnel due to tunnelling-induced ground settlement". Géotechnique, 60 (12), 927-938.

Muir-Wood, A.M., (1975). "The Circular Tunnel in Elastic Ground". Géotechnique, Vol. 25 (1) 115-127.

Nithiaraj, R., Ting, W.H., and Balasubramaniam, A.S. (1996). "Strength parameters of residual soils and application to stability analysis of anchored slopes". Geotechnical Engineering, 27, 55-81.

Ng, C.W.W., Boonyarak, T., and Masin, D. (2013). "Three-dimensional centrifuge and numerical modelling of the interaction between perpendicularly crossing tunnels". Canadian Geotechnical Journal, 50, 935-946.

Ng, C.W.W., Aye, Z.Z., Boonyarak, T., and Wang, R. (2017). "Three-dimensional interaction of multiple perpendicularly crossing tunnels with circular and horseshoe-shaped cross sections". Southeast Asian Conference and Exhibition in Tunnelling and Underground Space 2017 (SEACETUS 2017), Subang Jaya, Malaysia, 18-19 April 2017, pp 15-28.

Ooi, L. H., and Ha, T.T. (2016a) "The challenges of tunnelling works in Kuala Lumpur karsts". 19th Southeast Asian Geotechnical Conference & 2nd AGSSEA Conference (19 SEAGC & 2AGSSEA), Kuala Lumpur (31 May-3 June), pp 1151- 1158.

Ooi, L. H., and Ha, T.T. (2016b) "Deep excavations works in Kuala Lumpur karsts – some considerations". 19th Southeast Asian Geotechnical Conference & 2nd AGSSEA Conference (19 SEAGC & 2AGSSEA), Kuala Lumpur (31 May-3 June), pp 83- 90.

Ooi, T.A., Khoo, C.M. (2017). "Tunnelling activities in Malaysia- a review". Southeast Asian Conference and Exhibition in Tunnelling and Underground Space 2017 (SEACETUS 2017), Subang Jaya, Malaysia, 18-19 April 2017, pp. 243-252.

Peck, R.B., (1969). "Deep excavations and tunneling in soft ground". Proceedings of 7th Int. Conf. on Soil Mechanics and Foundation Engineering, 225-290.

Potts, D. M., (1976). "Behaviour of lined and unlined tunnels in sand". PhD thesis, Engineering Department, Cambridge University.

Poh, S.T., Low, Y.Y., Ooi, L.H. (2014). "Steel fibre reinforced concrete tunnel lining for a metro project – a Malaysian Experience". Proceedings of the 12th International Conference on Concrete Engineering and Technology (CONCET 2014), 87-94.

Poulos, H.G., and Deng, W. (2004). "An investigation on tunnelling-induced reduction of pile geotechnical capacity". Proc. 9th Australia-New Zealand Conf. On Geomechanics, Auckland, Vol. 1, 116-122.

Sagaseta, C. (1987). "Analysis of undrained soil deformation due to ground loss", Géotechnique 37, 301-320.

Schanz, T., Vermeer, P.A., and Bonnier, P.G. (1999). "Formulation and verification of the Hardening-Soil Model". In Beyond 2000 in Computational Geotechnics. R.B.J. Balkema Brinkgreve, Rotterdam. 281–290.

Tan, B.K. (2017). "Geology vis-à-vis tunnelling in the Kuala Lumpur Area". Southeast Asian Conference and Exhibition in Tunnelling and Underground Space 2017 (SEACETUS 2017), Subang Jaya, Malaysia, 18-19 April 2017, pp. 253-258.

Tan, J.G., Ooi, L.H., Yeoh, H.K. (2015). "Considerations of Deep Excavation in Kenny Hill and Kuala Lumpur Limestone Formations". International Conference and Exhibition on Tunnelling & Underground Space (ICETUS 2015), 3 – 5 March, Ooi T.A., Ooi, L.H. (Eds.), Tunnelling & Underground Space Division, The Institution of Engineers, Malaysia, 208-219.

Taniguchi, Y. (2010). "Construction of Vertically Parallel Twin Highway TBM-Driven Tunnels under Heavily-Congested Urban Subsurface Area in Tokyo". In Word Urban Transit Conference 2010, 20-22 October 2010, Sentosa, Singapore.

The British Tunnelling Society and The Institution of Civil Engineers (2010). "Specification for Tunnelling", Thomas Telford, 3rd Ed., 1-200.

Thewes, M., and Budach C. (2009). "Grouting of the annular gap in shield tunnelling – An important factor for minimisation of settlements and production performance", ITA-AITES World Tunnel Congress 2009, Safe Tunnelling for the City and Environment, 23-28 May.

Vaughan, P. R., Maccarini, M., Mokhtar, S. M. (1988). "Indexing engineering properties of residual soil". Quarterly Journal of Engineering Geology and Hydrogeology, 21, pp 69-84.

Vesic, A. B. (1961). "Bending of beams resting on isotropic elastic solids". J. Eng. Mech. Div. ASCE 87, 35-53.

Verruijt, A. and Booker, J.R., (1996). "Surface settlements due to deformation of a tunnel in an elastic half plane", Géotechnique, Vol. 46, No. 4, 753-756.

Wong, J. and Muhinder, S. (1996). "Some engineering properties of weathered Kenny Hill Formation in Kuala Lumpur", Proceedings of the 12th South East Asian Geotechnical Conference, 1, 179-187.

Yamaguchi, I., Yamazaki, I., and Kiritani, Y. (1998). "Study of ground-tunnel interactions of four shield tunnels driven in close proximity, in relation to design and construction of parallel shield tunnels". Tunnelling and Underground Space Technology, 13(3), 289-304.

Zhang, D., Huang, H., Phoon, K.K., and Hu, Q. (2014). "A modified solution of radial subgrade modulus for a circular tunnel in elastic ground". Soils and Foundations, 54(2), 225-232.